Supporting Information

Building Block Approach to Technetium-substituted Polyoxotungstates

Jenna Bustos[a], Lev N. Zakharov,[a] Jordi Buils[b,c], Farzaneh Hosseini,[b,c] Albert Solé-Daura,[b,c] Carles Bo[b,c*], May Nyman*[a]

[a]Department of Chemistry, Oregon State University, Corvallis, Oregon 97331 United States

[b]Institute of Chemical Research of Catalonia (ICIQ), Barcelona Institute of Science & Technology (BIST), Av. Països Catalans, 16, 43007 Tarragona, Spain

[c]Departament de Química Física i Inorgànica, Universitat Rovira i Virgili (URV), C/ Marcel·lí Domingo s/n, 43007 Tarragona, Spain

*Corresponding authors: may.nyman@oregonstate.edu

cbo@iciq.cat

Experimental Procedures

Caution! *Technetium-99 is a weak β-emitter (Emax = 292 keV). All manipulations were performed in a laboratory designed for work with radionuclides using HEPA filtered fume hoods and glovebox techniques while following locally approved radiochemistry handling and monitoring procedures.*

^{99}Tc was obtained from Oak Ridge National Laboratory as NH_4TcO_4. NH_4TcO_4 was purified and converted to $HTcO_4$ through a previously published procedure.[1] Briefly, 350 mg of NH_4TcO_4 is dissolved in 4 mL H_2O while stirring and heated to reflux. To the solution, 100 µL of 30% H_2O_2 was added to oxidize any black TcO_2 impurity. The cooled solution was then passed through a DOWEX 50WX8-100 cation exchange resin. The $HTcO_4$ eluate is collected and used. $Na_9[A\text{-}PW_9O_{34}]\cdot nH_2O$ and $Na_{10}[\alpha\text{-}SiW_9O_{34}]\cdot nH_2O$ were prepared following literature procedures, described briefly below.[2,3] All reagents and solvents were purchased from commercial suppliers and used as received.

Synthesis of $[Tc_2OCl_{10}]^{4-}$

In an argon filled glovebox, 100 µL of the $HTcO_4$ solution is added to a 4 mL vial. The uncapped vial is left to evaporate at room temperature yielding a red product of $H_4Tc_{20}O_{68}$ (Tc_{20}) after 2 days. The product is then dissolved in 3M HCl, which undergoes a color transformation from orange to green. The dark green solution indicates the presence of both $[Tc_2OCl_{10}]^{4-}$ and $[TcO_4]^-$ evidenced by UV-vis spectrophotometry (figure S1).

Synthesis of PW_9

$Na_9[\alpha\text{-}PW_9O_{34}]\cdot 7H_2O$ was prepared by dissolving 12 g of $NaWO_4$ in 15 mL of H_2O. Then 0.4 mL 85% H_3PO_4 was added dropwise with stirring. The pH is adjusted to 7 to 7.5 by addition of 2.25 mL of glacial acetic acid. A precipitate forms during the addition. After stirring for 1 h, the precipitate is collected and dried. This synthesis follows the previously reported procedure by Constant et. al.[2]

Synthesis of SiW_9

$Na_{10}[\alpha\text{-}SiW_9O_{34}]\cdot nH_2O$ was prepared by dissolving 1.1 g of Na_2SiO_3 in 20 mL of hot water. 18.2 g of $NaWO_4$ is then added with stirring. 13 mL of 6M HCl is then added dropwise. The solution is boiled until the volume is approximately 30 mL. A solution of 5 g Na_2CO_3 dissolved in 15 mL of water is then added

slowly with gentle stirring. The precipitate is filtered, stirred with 100 mL of 4M NaCl, then filtered and washed with ethanol and diethyl ether. The solid is dried under vacuum. This synthesis follows the previously reported procedure by Constant et. al.[3]

Synthesis of $K_4Tc_2OCl_{10}$

To the mixed $[Tc_2OCl_{10}]^{4-}$and $[TcO_4]^-$ solution prepared as stated above, 0.05 mL of 1 M KCl is added. The 4 mL glass vial is left open to evaporate. Orange-brown crystals of **$K_4Tc_2OCl_{10}$** appear after 2 days, co-crystallizing with $KTcO_4$.

Synthesis of Tc-POM-dimer

In a 4 mL glass vial, 12.3 mg of $Na_{10}SiW_9O_{34}{\cdot}nH_2O$ is dissolved in 490 µL of 0.1 M sodium acetate buffer at pH 5. Once dissolved, 10 µL of a mixed $[Tc_2OCl_{10}]^{4-}$and $[TcO_4]^-$ solution prepared as stated above was added to the POM solution and stirred. The solution turns from colorless to orange upon addition of the Tc solution, then gradually changes color to purple-red. The vial is left uncapped to evaporate. After 5 days, pink crystals of **Tc-POM-dimer** appear, co-crystallizing with other POM derivatives and Tc-substituted POM derivatives.

Synthesis of Tc-POM-chain

In a 4 mL glass vial, 12.2 mg of $Na_9PW_9O_{34}{\cdot}nH_2O$ is dissolved in 490 µL of 0.1 M sodium acetate buffer at pH 5. Once dissolved, 10 µL of a mixed $[Tc_2OCl_{10}]^{4-}$and $[TcO_4]^-$ solution prepared as stated above was added to the POM solution and stirred. The solution turns from colorless to orange upon addition of the Tc solution. After 1h, 10 µL of 5 M CsCl is added to the solution and the solution becomes cloudy. The vial is left uncapped to evaporate. After 5 days, colorless needle crystals of **Tc-POM-chain** appear, co-crystallizing with $H_3PW_{12}O_{40}$ and other POM derivatives and Tc-substituted POM derivatives.

Crystallographic Studies

All structures were collected at 173K using Rigaku Oxford SynergyS equipped with a PhotonJet S Cu source (λ=1.54178 Å) and hyPix-6000HE photon counting detector. All images were collected and processed using CrysAlisPro Version 171.40_64.53 (Rigaku Oxford Diffraction, 2018) [4]. After integration, both analytical absorption and empirical absorption (spherical harmonic, image scaling, detector scaling) corrections were applied [5]. Space groups were determined based on systematic absences (**$K_4Tc_2OCl_{10}$** and **Tc-POM-chain**) intensity statistics (**Tc-POM-dimer**). Absorption corrections were applied by SADABS.[5] Structures were solved by direct methods and Fourier techniques and refined on F^2 using full matrix least-squares procedures. [6,7.8] All non-H atoms were refined with anisotropic thermal parameters. Hydrogen atoms of lattice water molecules for **Tc-POM-dimer** and **Tc-POM-chain** were not located directly in the electron density map. Therefore, we can assume these water molecules are orientationally disordered, and only loosely associated in the lattice. However, two H atoms per water molecule were used in the calculation of crystal density (see **Table S1**). In addition, all structures were fully charge-balanced with countercations located in the electron density map, respectively Na^+ and Cs^+ for **Tc-POM-dimer** and **Tc-POM-chain**. Therefore, protonation of the POM oxygens was not required for charge-balance.

Additional comments about challenges with crystallographic data collection, treatment and refinement.

All three crystals used for data collections were twins consisting of two domains. All three structures were determined and refined based on the HKLF4 sets that include reflections related only to one domain. These HKLF4 files provide an appropriate number of reflections per the number of the refined parameters: 297/20 (**$K_4Tc_2OCl_{10}$**), 7017/702 (**Tc-POM-dimer**) and 4680/358 (**Tc-POM-chain**). The HKLF5 sets did not improve the final data. The Fractal Dimension and Fobs_Fcalc plots for all three structures (respectively **figures S3** and **S4**) show that the quality of the final XRD data are not perfect. Twinning in these crystals appears to be more complicated than the current models depict (i.e. additional small domains).

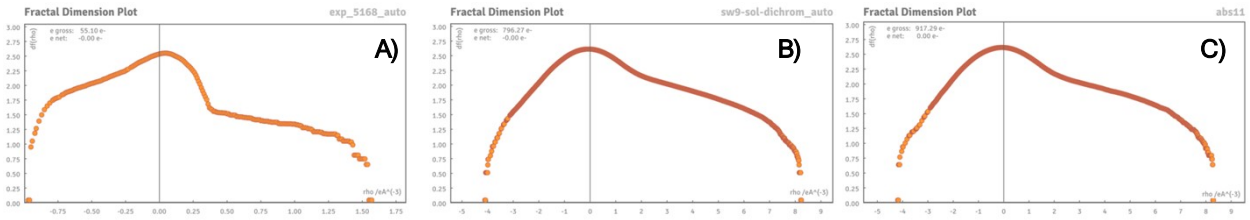

Figure S1. Fractal dimension plots for A) $[Tc_2OCl_{10}]^{4-}$, B) Tc-POM-dimer and C) Tc-POM chain.

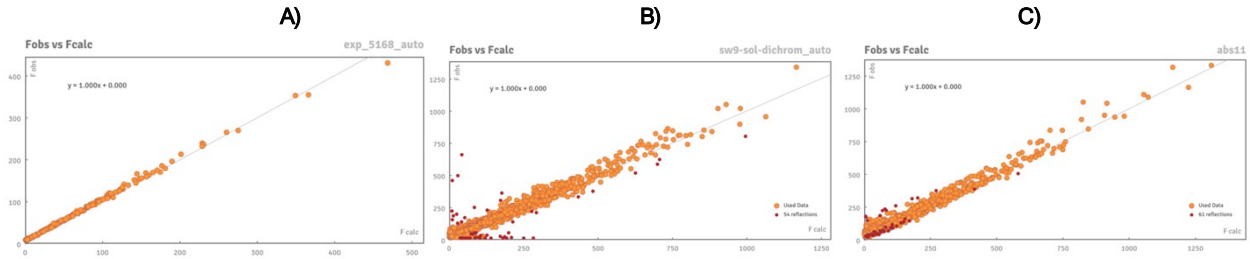

Figure S2. F_{obs} vs. F_{calc} plots for A) $[Tc_2OCl_{10}]^{4-}$, B) Tc-POM-dimer and C) Tc-POM chain.

The diffraction data for **Tc-POM-dimer** were collected up to $2\theta_{max} = 151.01°$, but only reflections up to 120.0° were used in the final refinement. The RIGU option was used for the refinement of **Tc-POM-dimer**. There are relatively high peaks on the residual density maps for **Tc-POM-dimer** and **Tc-POM-chain,** but these are located close to heavy W metal atoms, typical for structures containing multiple heavy atoms. There are several weaker peaks indicating additional possible positions for partially occupied solvent water molecules (**figure S5**). Some disordered solvent water molecules were identified and treated in the current models with partial occupancy. However, the network of water molecules in these structures seems to be more complex than represented in the current models.

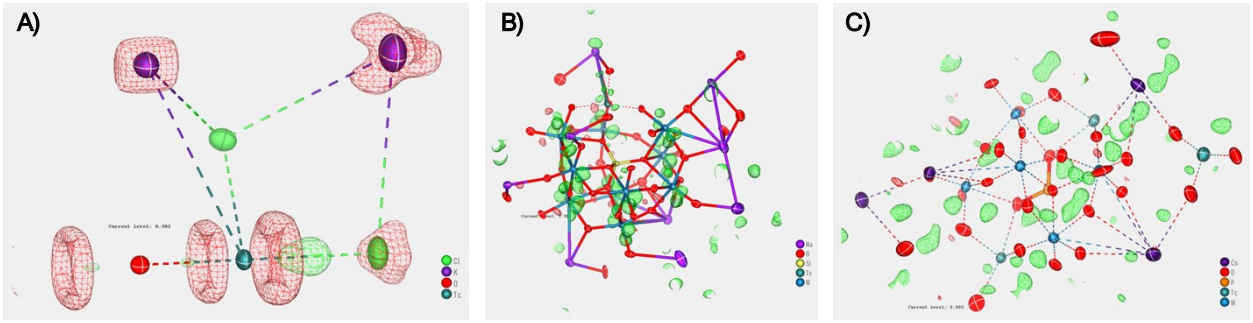

Figure S3. Representative residual electron density maps for A) $[Tc_2OCl_{10}]^{4-}$, B) Tc-POM-dimer and C) Tc-POM chain.

Table S1. Crystallographic Information of the Isolated Structures			
Identification Code	**$K_4Tc_2OCl_{10}$**	**Tc-POM-dimer**	**Tc-POM-chain**
CCDC	2500437	2500439	2500438
Empirical formula	$Cl_{10}K_4OTc_2$	$H_{70}Na_{16}O_{95}Si_2Tc_2W_{20}$	$Cs_7H_{18}O_{52}PTc_3W_{10}$
Moiety formula	$K_4[Tc_2OCl_{10}]$	$Na_{14}[Na_2(H_2O)_4Tc_2O_2(\alpha\text{-}SiW_{10}O_{37})_2]\cdot 35H_2O$	$Cs_7(Tc^{VI}O_4)$*trans*-$[Tc^{IV}_2PW_{10}O_{39}]\cdot 9H_2O$
Formula weight	722.92	5887.30	3943.82
Temperature/K	173.00(10)	172.99(11)	173.00(11)
Crystal system	tetragonal	triclinic	monoclinic
Space group	*I4/mmm*	*P*-1	$P2_1/m$
a/Å	7.026(13)	11.1676(3)	11.466(4)
b/Å	7.026(13)	13.2240(5)	18.3654(5)
c/Å	17.55(4)	17.8381(4)	12.9591(4)
α/°	90	105.761(3)	90
β/°	90	93.878(2)	105.187(2)
γ/°	90	107.976(4)	90
Volume/Å^3	866 (4)	2383.30(13)	2606.18(15)
Z	2	1	1
ρ_{calc} g/cm^3	2.771	4.111	5.026
μ/mm^{-1}	35.621	47.644	84.699
F(000)	680.0	2600.0	3406.0
Crystal size/mm^3	0.06 × 0.06 × 0.04	0.06 × 0.03 × 0.01	0.11 × 0.02 × 0.01
Radiation	Cu Kα (λ = 1.54184)	Cu Kα (λ = 1.54184)	Cu Kα (λ = 1.54184)
2Θ range for data collection/°	10.066 to 148.81	7.614 to 152.142	7.066 to 148.886
Index ranges	$-4 \le h \le 7$, $-8 \le k \le 8$, $-21 \le l \le 21$	$-14 \le h \le 13$, $-16 \le k \le 15$, $-22 \le l \le 20$	$-13 \le h \le 14$, $-19 \le k \le 22$, $-16 \le l \le 14$
Reflections collected	1049	24029	25612
Independent reflections	297 [R_{int} = 0.0257, R_{sigma} = 0.0145]	7012 [R_{int} = 0.1019, R_{sigma} = 0.0888]	5422 [R_{int} = 0.0708, R_{sigma} = 0.0443]

Data/parameters	297/20	7012/702	4680/358
Goodness-of-fit on F^2	1.009	1.033	1.060
Final R indexes [I>=2σ (I)]	R_1 = 0.0320, wR_2 = 0.0778	R_1 = 0.0996, wR_2 = 0.2351	R_1 = 0.0942, wR_2 = 0.2529
Final R indexes [all data]	R_1 = 0.0279, wR_2 = 0.0677	R_1 = 0.1030, wR_2 = 0.2453	R_1 = 0.0991, wR_2 = 0.2493
Largest diff. peak/hole / e $Å^{-3}$	1.133/-1.071	6.596/-1.826	3.468/-2.598

Table S2. Bond Valence Sum (BVS) calculations for $K_4Tc_2OCl_{10}$

Atom 1	Atom 2	Bond distance (Å)	Bond valence	Atom (BVS), attribution
Tc1	O1	1.850	0.975969	Tc1 (4.126), Tc^{IV}
	Cl1	2.380	0.631625	
	Cl1	2.380	0.631625	
	Cl1	2.380	0.631625	
	Cl1	2.380	0.631625	
	Cl2	2.385	0.623147	

$^1R_{0\ (Tc\text{-}O)}$ = 1.841 b= 0.37 [9], $R_{0\ (Tc\text{-}Cl)}$ = 2.21 b= 0.37 [*]

*BV parameter obtained from IUCr database listed without a reference article. BV parameters accessed at: https://www.iucr.org/resources/data/datasets/bond-valence-parameters

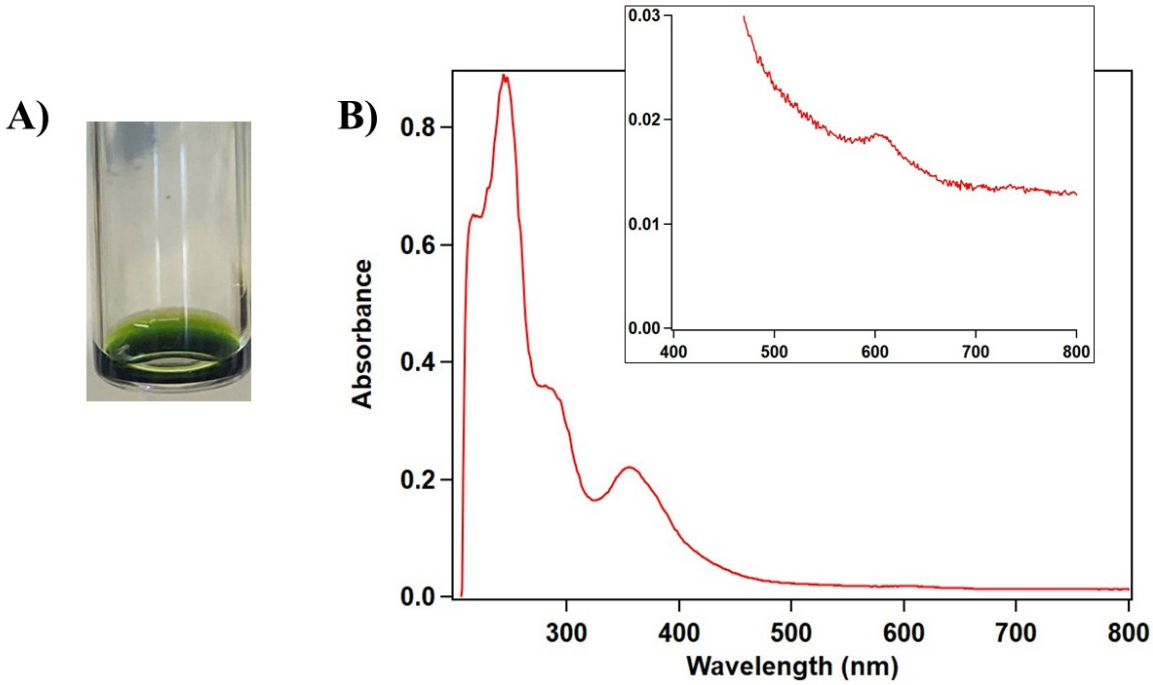

Figure S4. A) Image of green solution obtained by dissolution of Tc_{20} in 3M HCl. B) Absorbance spectrum of the mixed $[Tc_2OCl_{10}]^{4-}$ and $[TcO_4]^-$ solution. The inset shows the small peak at 607 nm. Peaks at 244 and 287 nm are characteristic of TcO_4^- and the peaks at 358 and 607 nm are attributed to $[Tc_2OCl_{10}]^{4-}$.

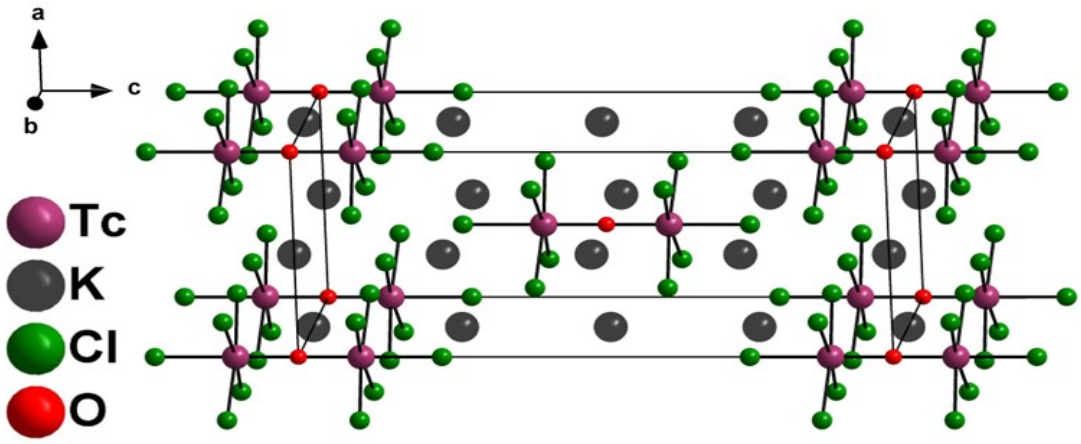

Figure S5. Lattice arrangement of $K_4Tc_2OCl_{10}$ as viewed down the *ab* axis

Computational Details

The molecular geometries of the technetium complexes were fully optimized using the ADF[10] software package (SCM ADF versions 2021.101 and 2023.101) using the PBE[11] functional. Relativistic effects were considered using the scalar-relativistic zero-order regular approximation[12,13] (ZORA) to address the influence of heavier elements. A Triple-Zeta Polarization (TZP) basis set was employed to provide an adequate description of the molecular orbitals. Solvation effects were considered using the Conductor-like Screening Model (COSMO), considering water as solvent with the Klamt[14] radii for water. The calculations utilized a Core Large approach, facilitating a more accurate representation of the core electrons particularly for heavy atoms. A dataset collection with all DFT calculations is available in the ioChem-BD[15] repository through this link https://iochem-bd.iciq.es/browse/review-collection/100/108159/0117aa0587cd8413a017c376

Table S3

DFT computed geometric parameters and bonding energies for some electronic states of $[Tc_2OCl_{10}]K_4$

		X-Ray	Singlet	Triplet	Septet
Distance (Å)	Tc-O	1.850(4)	1.88	1.84	1.98
Angle (º)	Tc-O-Tc	180.0(0)	180	180	180
Energy (kcal.mol^{-1})	-	-	-1651.58	-1643.84	-1635.54

DFT computed geometric parameters and bonding energies for some electronic states of $[Tc_2OCl_{10}]^{4-}$

		X-Ray	Singlet	Triplet	Septet
Distance (Å)	Tc-O	1.850(4)	1.82	1.82	1.94
Angle (º)	Tc-O-Tc	180.0(0)	180	180	180
Energy (kcal.mol^{-1})	-	-	-1700.13	-1711.58	-1698.15

Table S4. Bond Lengths for Tc-POM-dimer						
Atom	Atom	Length/Å		Atom	Atom	Length/Å
W1	O00U	2.083(17)		Na1	O00O	2.612(19)
W1	O00Y	1.953(18)		Na1	O00O^{4}	2.612(19)
W1	O018	1.724(17)		Na1	O013	2.624(19)
W1	O01C	2.273(17)		Na1	O013^{4}	2.624(19)
W1	O01H	1.771(18)		Na1	O016^{4}	2.712(19)
W1	O200	1.931(18)		Na1	O016	2.712(19)
W2	O01J	1.926(18)		Na1	O01J^{4}	2.640(17)
W2	O00O	1.990(19)		Na1	O01J	2.640(17)
W2	O00P	1.73(2)		Na7	O00X	2.99(3)
W2	O01B	1.822(18)		Na7	O01F	2.30(2)
W2	O01E	1.924(19)		Na7	O01S	2.37(3)
W2	O01G	2.355(18)		Na7	O01T	2.30(3)
W3	O01G	2.321(17)		Na7	O2S	2.46(3)
W3	O00K	1.907(18)		Na7	O100	2.31(3)
W3	O00T	1.997(18)		Na8	O00R	2.34(2)
W3	O01M	1.730(18)		Na8	O00S^{2}	2.52(2)
W3	O01E	1.954(19)		Na8	O00X	2.29(2)
W3	O00U	1.824(18)		Na8	O00Y^{5}	2.75(2)
W4	O01P	1.693(19)		Na8	O018^{5}	2.93(2)
W4	O00O	1.91(2)		Na8	O01T	2.46(3)
W4	O00T	1.872(19)		Na8	O01U	2.55(3)
W4	O013	1.894(19)		Na9	O00R	2.40(2)
W4	O01G	2.317(17)		Na9	O00S^{2}	2.53(2)
W4	O01I	1.917(18)		Na9	O01H^{5}	2.36(2)
W5	O200	1.909(18)		Na9	O01N	2.40(2)
W5	O00K	1.922(17)		Na9	O01O^{2}	2.46(3)
W5	O00S	1.713(19)		Na9	O3S	2.49(4)
W5	O01A	2.387(17)		Na6	O017	2.38(3)
W5	O01D	1.954(18)		Na6	O01P^{4}	2.38(3)
W5	O01K	1.869(16)		Na6	O2S	3.10(4)
W6	O00V	1.898(18)		Na6	O100	2.41(4)
W6	O00W	2.340(18)		Na6	O102	2.40(5)
W6	O016	1.925(19)		Na6	O121	2.46(8)
W6	O017	1.70(2)		Na2	O00P	2.96(4)
W6	O01F	1.877(18)		Na2	O019^{4}	3.09(4)
W6	O01J	1.931(17)		Na2	O01P^{4}	3.05(4)
W7	O00L	1.72(2)		Na2	O111	2.63(5)
W7	O010	1.910(19)		Na2	O112	2.40(5)

W7	O015	1.838(18)		Na2	O113	2.81(7)
W7	O01A	2.442(18)		Na2	O121	2.45(8)
W7	O01D	1.944(18)		Na4	O00M[2]	2.34(2)
W7	O01I	1.929(18)		Na4	O00N	2.26(2)
W8	O00M	1.777(18)		Na4	O014[2]	2.37(2)
W8	O00V	1.929(18)		Na4	O015	3.01(2)
W8	O00Y	1.929(17)		Na4	O01C[2]	3.04(2)
W8	O011	1.79(2)		Na4	O01H[2]	2.39(2)
W8	O01B	2.100(17)		Na4	O01N[6]	2.46(2)
W8	O01C	2.233(18)		Na4	O01R	2.65(3)
W9	O00Q	2.090(18)		Na3	O00P	2.30(2)
W9	O00W	2.368(17)		Na3	O019[4]	2.38(2)
W9	O00X	1.735(19)		Na3	O01E[7]	2.39(2)
W9	O012	1.872(19)		Na3	O01Q[7]	2.47(3)
W9	O014	1.743(19)		Na3	O01Q	2.38(2)
W9	O01F	2.023(19)		Na3	O103	2.29(4)
W10	O00Q	1.841(18)		Na5	O01H	2.58(2)
W10	O00W	2.399(18)		Na5	O012	2.37(2)
W10	O010	1.909(19)		Na5	O00N	2.54(2)
W10	O013	1.975(18)		Na5	O200	2.48(2)
W10	O016	1.94(2)		Na5	O018	2.29(2)
W10	O019	1.723(18)		Na5	O01K	2.66(2)
Tc1	Tc1[2]	2.398(4)		Na5	O01O	2.35(2)
Tc1	O00N[2]	1.938(18)		Na5	O01H	2.58(2)
Tc1	O00N	1.916(17)		Si1	O00W	1.635(19)
Tc1	O012	1.949(18)		Si1	O01A	1.631(19)
Tc1	O015	2.047(18)		Si1	O01C	1.619(18)
Tc1	O01A	2.181(17)		Si1	O01G	1.675(18)
Tc1	O01K	2.014(17)				

[1]2-X,1-Y,1-Z; [2]1-X,1-Y,1-Z; [3]1+X,+Y,+Z; [4]1-X,1-Y,-Z; [5]-1+X,+Y,+Z; [6]-X,1-Y,1-Z; [7]2-X,1-Y,-Z

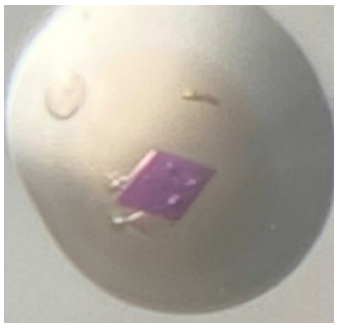

Figure S6. Single crystal of **Tc-POM-dimer**

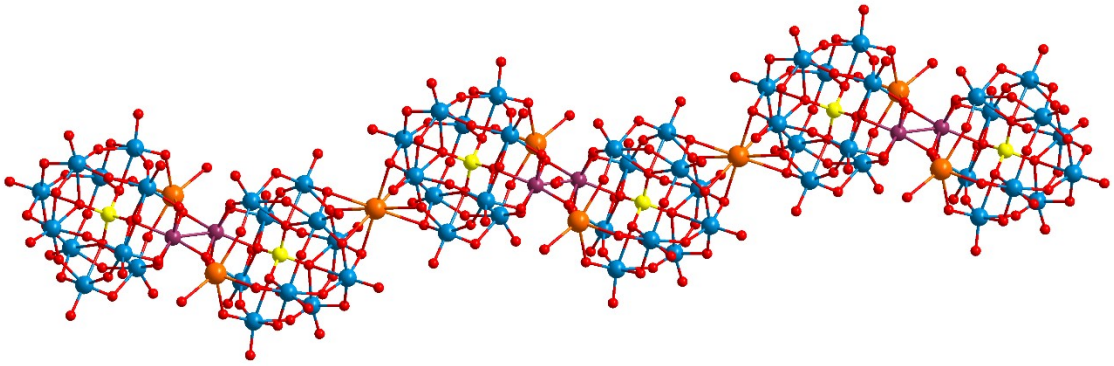

Figure S7. **Tc-POM-dimer** connecting through Na^+ cations along *c* axis. Blue is W, purple is Tc, yellow is Si, orange is Na, and red is O.

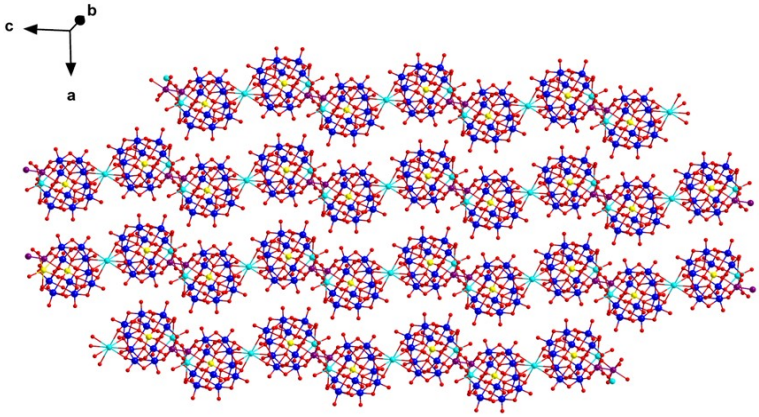

Figure S8. Stacking sequence of **Tc-POM-dimer** chains down the *a*-axis. Blue is W, purple is Tc, turquoise is Na, yellow is Si, and red is O.

Table S5. Structures containing the $[Tc_2O_2]^{4+}$ core			
Ligand	Structure	Tc-Tc Bond Distance (Å)	ref
EDTA	$Tc_2O_2(H_2EDTA)_2$	2.33	[16]
NTA	$Na_2Tc_2O_2(NTA)_2$	2.36	[17]
Ox	$K_4Tc_2O_2(C_2O_4)_4$	2.36	[18]
TCTA	$Ba_2Tc_2O_2(TCTA)_2ClO_4 \cdot 9H_2O$ (mixed (III/IV)) $[Tc_2O_2]^{3+}$ core	2.40	[19]
SiW_{10}	$Na_{14}[Na_2(H_2O)_4Tc_2O_2$ $(\alpha\text{-}SiW_{10}O_{37})_2] \cdot 35H_2O$	2.40	This work
TCTA= 1,4,7-Triazacvclononane-N, N', N",-triacetate EDTA= ethylenediaminetetraacetate NTA= nitrilotriacetate Ox= oxalate			

Table S6. Computed Bonding Energy and Tc-Tc bond distances for singlet and triplet electronic states of the **Tc-POM-dimer** $Na_2O_{76}Si_2Tc_2W_{20}$

	Energy (kcal.mol^{-1})	Tc-Tc distance (Å)
Singlet	-20498.48	2.395
Triplet	-20497.52	2.553
Quintet	-20485.48	2.577
Experimental	—	2.398

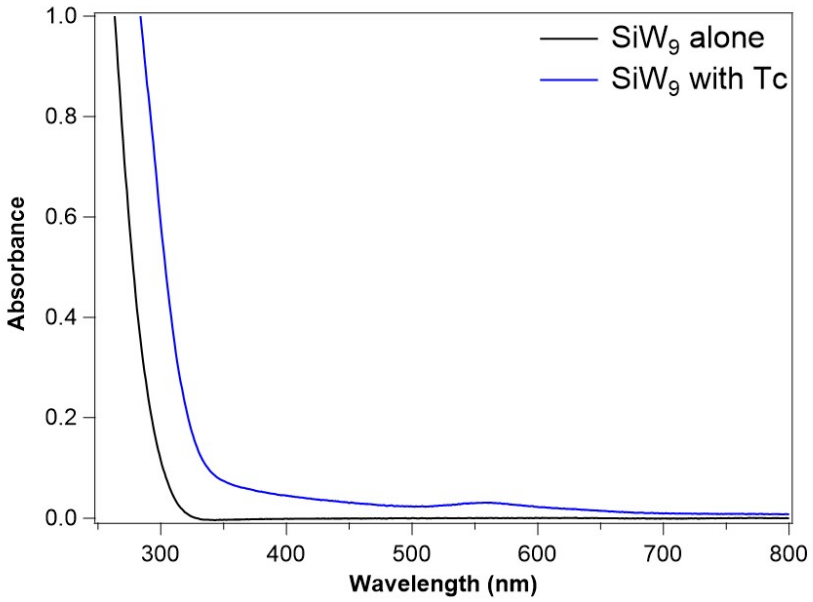

Figure S9. Absorbance of POM with (blue) and without (black) Tc. The absorbance of the POM shifts with addition of the mixed $[Tc_2OCl_{10}]^{4-}$ / TcO_4^- solution.

Small Angle X-ray Scattering (SAXS). SAXS data were collected on an Anton Parr SAXSess instrument utilizing Cu-Ka radiation and line collimation. Data was recorded on an image plate in the range of 0.08-2.5 $Å^{-1}$. The sample to image plate distance is 26.1 cm. For safety, solutions containing Tc were measured in 1.5 mm Kapton polyamide tubes (Cole-Palmer). The Kapton tubes were cut to the desired length and sealed on one end using epoxy. The Kapton tubes were sealed on the open end with wax. Water in a Kapton tube was used as a background and scattering was measured for 30 minutes. SAXSQUANT software was used for data collection and processing (normalization, primary beam removal, and background subtraction). IRENA30 macros within IGOR Pro[20] was used for data analysis. Simulated scattering curves of SiW_9, SiW_{11}, and $(SiW_{10}Tc)_2$ were generated using SolX[21] utilizing structural files of NaH_3SiW_{12}[22] and Tc-POM-dimer (.xyz).

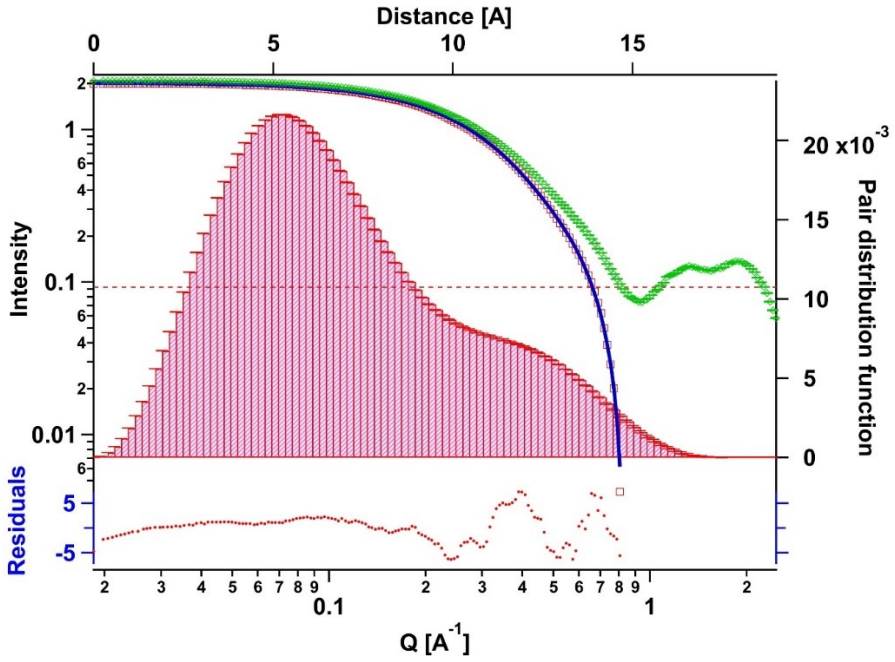

Figure S10. Pair distance distribution function for **Tc-POM-dimer** reaction solution. Data was fit using Moore's indirect Fourier transform [23] with a maximum extent of 17.6 Å and R_g of 5.40 Å. The simulated scattering of **Tc-POM-dimer** yields an R_g of 5.9 Å, and simulated scattering for SiW_{11} exhibits an R_g of 3.67 Å. The experimental R_g is consistent with a mixture of (mostly) dimer complexes and uncomplexed POM. Green is the experimental scattering curve. Red squares are the scattering data range that was used for the data analysis, minus the flat background. Solid blue line is a fit to this data range, horizontal dashed red line is the subtracted flat background, bar graph is the PDDF result. The red dots (bottom) are the residua of the data-model fit.

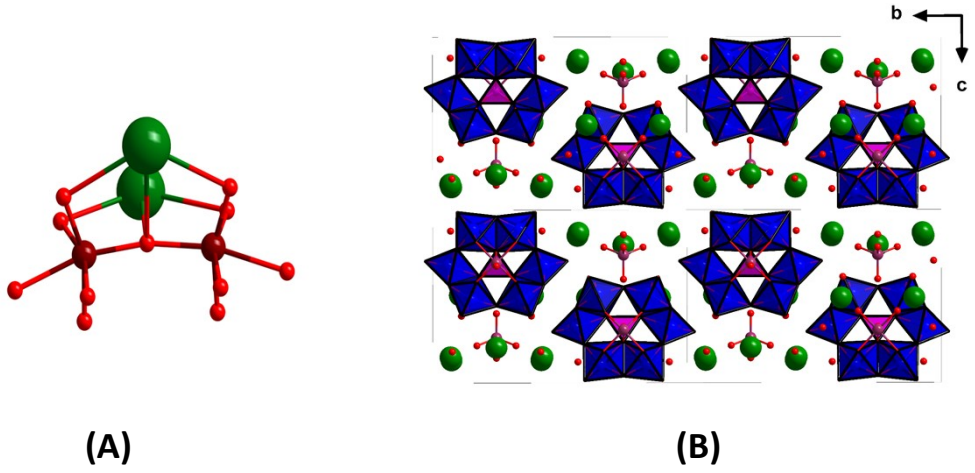

Figure S11. Two Cs+ cations coordinating the Tc_2O core of the **Tc-POM-chain** structure. Cs is green, Tc is purple, and O is red.

Table S7. Bond valence sum (BVS[1]) calculations for Tc-POM-chain				
Atom 1	Atom 2	Bond distance (Å)	Bond valence	Atom (BVS), attribution

Tc3	O2	1.98	0.825396	Tc1 (4.13), $Tc^{III/IV}$
	O2	1.98	0.825396	
	O20	2.025	0.730875	
	O20	2.025	0.730875	
	O00N	2.46	0.225555	
	O50	1.995	0.792603	
Tc5	O30	2.454	0.229243	Tc2 (3.59), $Tc^{III/IV}$
	O50	2.256	0.391473	
	O00P	1.98	0.825396	
	O00P	1.98	0.825396	
	O00V	2.063	0.659538	
	O00V	2.063	0.659538	
Tc4	O21	1.729	1.626591	Tc3 (6.37), $Tc^{VII/VI}$
	O22	1.756	1.512121	
	O00T	1.731	1.617822	
	O00T	1.731	1.617822	
$^{1}R_{0\ (Tc\text{-}O)}$ = 1.909 b= 0.37 [12], parameters for 7+ were used for all Tc atoms				

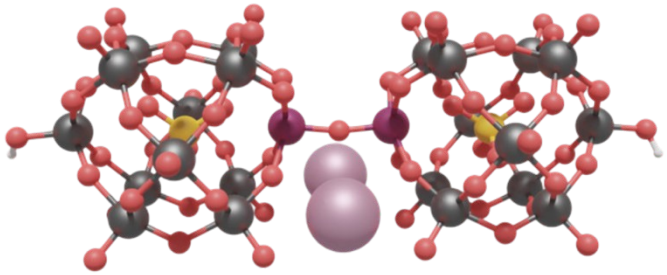

Figure S12. Molecular structure of the simplest cluster model for the **Tc-POM-chain** material HO-Keg-Tc-O-Tc-Keg-OH, named *simple model*. Note that only two Tc atoms were included, which are those that form the Tc-O-Tc bridge. The two Cs cations closest to the bridge in the X-Ray structure were also included and located at the crystallographic positions. A more realistic model of the X-Ray structure, which included the four Tc atoms, named *crystal model* HO-Tc-Keggin-Tc-O-Tc-Keggin-Tc-OH were also considered. Color code: Oxygen: red; Technetium: deep purple; Phosphorus: orange-yellow; Tungsten: metallic gray; Cesium: metallic lavender; Spin densities: sky blue and vermilion (orangish).

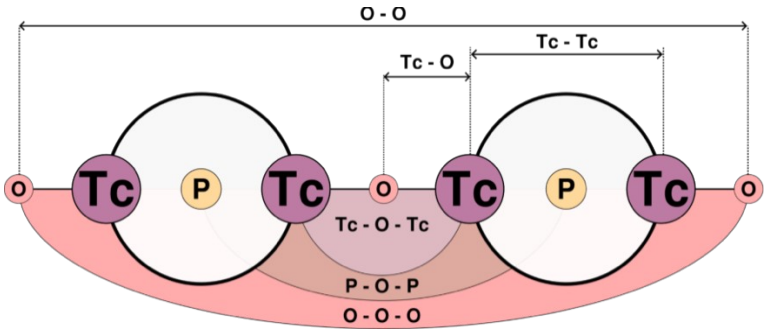

Figure S13. Definition of the geometrical parameters' measurements included in **Tables S8** and **S9**.

Table S8. Geometrical parameters for the most stable structures and electronic states for the simple model HO-Keg-Tc-O-Tc-Keg-OH.

		Computational							
		Exp.		Tc(III) Singlet		Tc(III)/Tc(IV) Doublet		Tc(IV) Singlet	
Distances (Å)	Tc-O	2.17	2.07	1.87	1.87	1.86	1.92	1.92	1.86
	Tc-W	7.15		7.46	7.47	7.41	7.50	7.46	7.50
	O-O	11.36		11.27	11.27	11.29	11.25	11.27	11.25
Angles (º)	Tc-O-Tc	167.42		169.54		168.25		168.24	
	P-O-P	175.91		179.37		178.58		178.58	
	O-O-O	180.00		178.95		179.60		179.60	

Table S9. DFT results on HO-Tc-Keggin-Tc-O-Tc-Keggin-Tc-OH (crystal model)

		Computational							
		Exp.		Tc(III) Nonaplet		Tc(III)/Tc(IV) Singlet		Tc(IV) Singlet	
Distances (Å)	Tc-O	2.17	2.07	2.03	2.02	1.91		1.95	1.94
	Tc-Tc	7.15		7.26	7.27	7.35		7.33	7.32
	O-O	11.36		11.36	11.36	11.35		11.36	11.35
Angles (º)	Tc-O-Tc	167.42		153.70		170.60		168.30	
	P-O-P	175.91		171.80		179.90		178.90	
	O-O-O	180.00		176.10		178.90		179.80	

Table S10. DFT results on HO-Tc-Keggin-Tc-O-Tc-Keggin-Tc-OH (crystal model)

		Tc(III)	
Spin Multiciplity	S=17	S=9	S=1 (error)
Rel. Energy ($kcal.mol^{-1}$)	11.99	0	----

			Tc(III)/Tc(IV)					
Spin Multiciplity	S=15	S=13	S=11	S=9	S=7	S=5	S=3	S=1
Rel.Energy $kcal.mol^{-1}$	Geom Broken	Geom Broken	11.57	---	Geom Broken	10.9	3.55	0

		Tc(IV)	
Spin Multiciplity	S=13	S=7	S=1
Rel. Energy ($kcal.mol^{-1}$)	9.07	0.31	0

S = 13

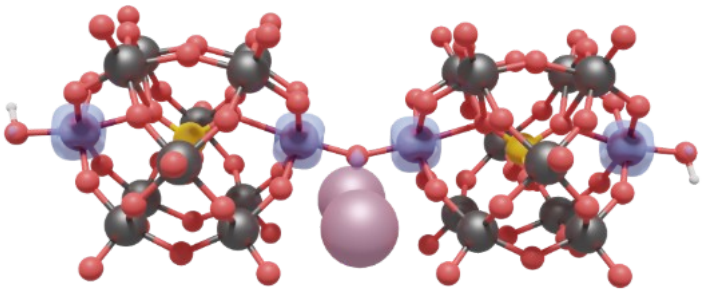

S = 7

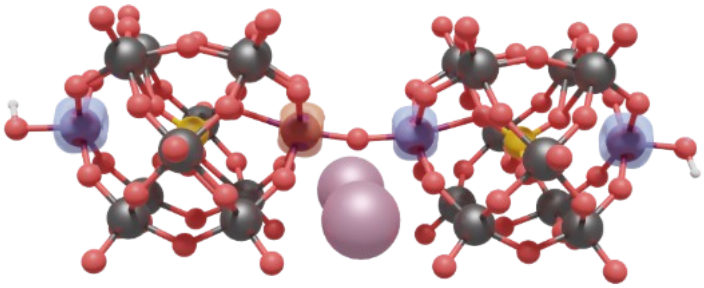

S = 1

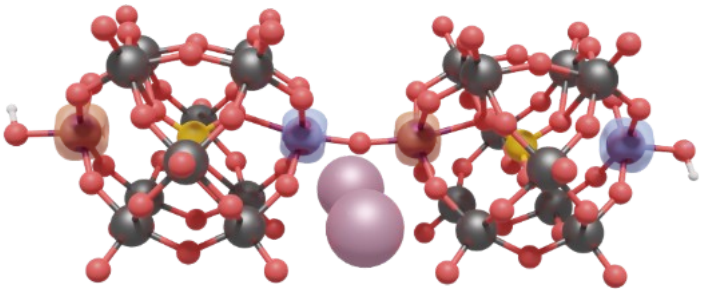

Figure S14. Spin Density Maps for some electronic states of the crystal model HO-Tc-Keggin-Tc-O-Tc-Keggin-Tc-OH. Color code: Oxygen: red; Technetium: deep purple; Phosphorus: orange-yellow; Tungsten: metallic gray; Cesium: metallic lavender; Spin densities: sky blue and vermilion (orangish).

Simulations of TcO_4^- and TcO_4^{2-} for Tc-POM-chain

Table S11. Tc(VI)

	Bonding Energy (Kcal.mol^{-1})	**Rel Energy (Kcal.mol^{-1})**
TcO_4^{2-} C_{2V}	-1052.57	0
TcO_4^{2-} Crystal	-1052.07	0.5

Table S12. Tc(VII)

	Bonding Energy (Kcal.mol^{-1})	**Rel Energy (Kcal.mol^{-1})**
TcO_4^- Td	-997.60	0
TcO_4^- Crystal	-997.25	0.35

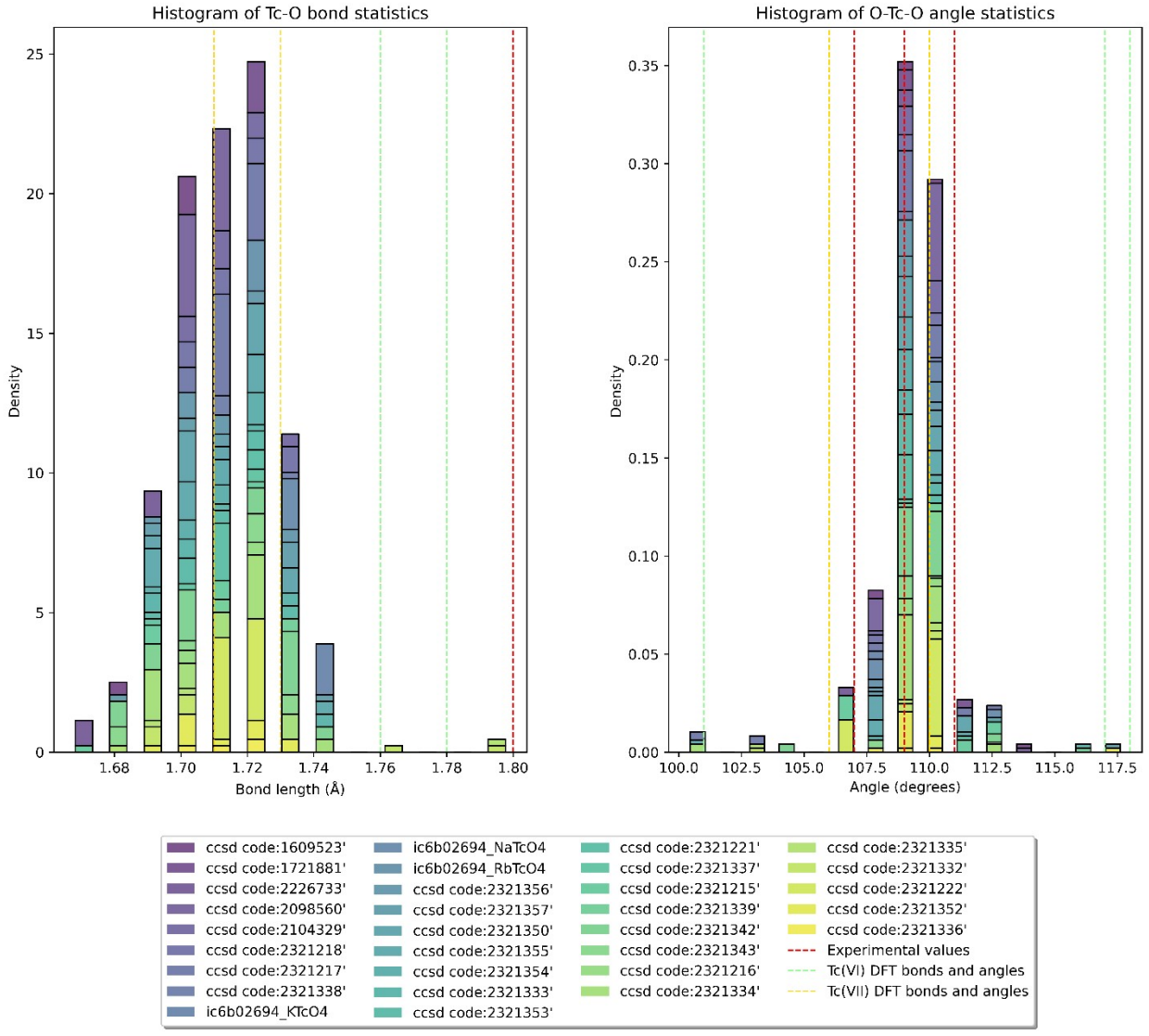

Figure S15. Summation of Tc-O bonds (Å) and O-Tc-O angles (º) for TcO_4^- containing structures reported in the literature, compared to that for **Tc-POM-chain**. The structure codes are listed as 'ccsd' (Cambridge Crystallographic Database) or 'ic' (ICSD) are those given in the archived files in the CCDC.

References

[1] M. Shohel, J. Bustos, G. D. Stroscio, A. Sarkar and M. Nyman. *Inorg Chem* 2023, 62, 10450-10460.
[2] Domaille, P. J.; Hervéa, G.; Téazéa, 1990, 27, 96–104.
[3] A. Téazéa, G. Hervéa, R. G. Finke and D. K. Lyon, 1990, 27, 85–96.
[4] SAINT, version 8.34A, Bruker AXS Inc., Madison, WI, 2013
[5] G. M. Sheldrick, *Bruker/Siemens Area Detector Absorption Correction Program*, Bruker AXS, Madison, WI, 1998.
[6] G. Sheldrick, Acta Cryst A 2015, 71, 3-8.
[7] G. Sheldrick, Acta Crystal A 2008, 64, 112-122.
[8] O. V. Dolomanov, L. J. Bourhis, R. J. Gildea, J. A. K. Howard and H. Puschmann, *J Appl Cryst* 2009, 42, 339-341.
[9] D. W. Wester and N. J. Hess, Inorganica Chim. Acta, 2005, 358, 865–874.
[10] G. Te Velde, F. M. Bickelhaupt, E.J. Baerends, C. Fonseca Guerra, S. J. A. Van Gisbergen, J. G. Snijders, T. Ziegler. *J Comput Chem* **2001**, 22 (9), 931–967.

[11] P. Perdew, K. Burke, M. Ernzerhof, *Phys. Rev. Lett.* 77, 3865-3868 (1996)], Phys. Rev. Lett. 78 (1997) 1396–1396.
[12] E. Van Lenthe, E. J. Baerends. *J Comput Chem* **2003**, 24 (9), 1142–1156.
[13] E. V Lenthe, E. J. Baerends, J. G. Snijders. *J. Chem. Phys.* **1993**, 99 (6), 4597–4610.
[14] A. Klamt. *J. Phys. Chem.* **1995**, 99, (7), 2224-2235.
[15] M. Álvarez-Moreno, C. De Graaf, N. López, F. Maseras, J. M. Poblet, C. Bo, *J. Chem. Inf. Model.* **2015**, 55 (1), 95–103.
[16] H.B. Buergi, G. Anderegg, P. Blaeuenstein, Inorg. Chem., 1981, 20, 3829–3834.
[17] G. Anderegg, E. Miiller, K. Zollinger and B. Hans-Beat, Helv. Chim. Acta, 1983, 66, 1593–1598.
[18] Alberto, R., Anderegg, G. and Albinati, A., 1990. *Inorganica chimica acta*, *178*(1), pp.125-130.
[19] K. E. Linder, J. C. Dewan and A. Davison, Inorg. Chem., 1989, 3820–3825.
[20] J. Ilavsky, P. R. Jemian, J. Appl. Crystallogr. 2009, 42 (2), 347–353.
[21] X. Zuo, G. Cui, K. M. Merz, L. Zhang, F. D. Lewis and D. M. Tiede, PNAS 2006, 103, 3534-3539.
[22] C. S. Wu, B. S. Zhang, J. P. Qiu and Y. X. Li, J. Coord. Chem., 2014, 67, 3454–3462.
[23] P. B. Moore, *J. Appl. Crystallogr.* 1980, **13** (2), 168–175.